

АКАДЕМИЯ НАУК
СССР

ACADEMY OF SCIENCES
USSR

ИНСТИТУТ
ПРОБЛЕМ БЕЗОПАСНОГО
РАЗВИТИЯ ЯДЕРНОЙ ЭНЕРГЕТИКИ

NUCLEAR
SAFETY INSTITUTE

Preprint N 17

Arutjunjan R.V., Bolshov L.A., Varenkov V.V.,
Goloviznin V.M., Kanukova V.D., Popkov A.G.,
Strizhov V.F., Chudanov V.V., Shipovskikh T.A.

MODELING OF SURC-4 EXPERIMENTS

Arutjunjan R.V., Bolshov L.A., Varenkov V.V.,
Goloviznin V.M., Kanukova V.D., Popkov A.G.,
Strizhov V.F., Chudanov V.V., Shipovskikh T.A.

MODELING OF SURC-4 EXPERIMENTS THERMOHYDROLOGICS. -
Preprint / Institute of Nuclear Safety Academy of Sciences of the
USSR, - Moscow: 1991. N

ABSTRACT

Thermophysics of SURC-4 experiments on molten core concrete interaction studies is analysed by means of CORCON and RASPLAV codes. The main attention is paid for modeling of heat losses in the specific one dimensional experimental geometry. The experimental and calculated results are compared. It is shown that chemical heat production play important role in this experiment and to reach good agreement it is necessary to consider carefully the zirconium chemistry in melt.

1. Introduction

In risk assessment for the NPP with light water reactors, the accidents with the core melt are of great importance. In spite the probability of such accidents is low, their consequences may be rather severe due to the considerable radioactivity release when the primary circuit is failed. In the course of the accident with the core melt it is quite probable the long term interaction of the molten fuel and constructional materials with concrete. Such interaction is extremely undesirable, due to the significant increase of pressure under the containment, increase of the atmospheric temperature, possible basemat melting through, the radioactive contamination of the area and ground water. That's why the great attention is spared for the analysis of the processes molten/concrete interaction (MCI).

The research work, concerning these problems is performed worldwide and includes a wide range of problems, beginning from the thermal processes analysis in the course of MCI and to the radioactivity release. In some research centers, such as SANDIA [1] in the USA, KFK in FRG [2] and some others, the experiments, concerning the interaction of the melt, simulating the core, with concrete are performed. The goal of these experiments is, on one hand, the receipt the experimental information about the materials behavior during the MCI and, on the other hand, all these investigations allow to verify the computers programs, developed for the MCI analysis.

The main processes which are to be modeled, while analyzing the MCI may be divided into three groups:

- thermal-hydraulic processes, including heat balance of the molten core (MC) during the interaction, various processes of heat transfer between separate molten components with the account of phase transition of the molten components and etc;

- chemical reactions between the molten components and the products of concrete decomposition; these processes are closely connected with processes of generation and aerosol release;
- the change of the molten geometry and and the interface between the melt and concrete in the process of decomposition.

The separate problem is the development of models for calculation of thermal-physical properties of the melt components with the account of its composition.

The variety of process, taking place during the interaction of the molten fuel with concrete, the absence of detailed information in many cases, result in variety of approaches in developing numerical models and programs. Today, several programs for modeling the processes of melt/concrete interaction are used (for instance CORCON [3], WECHSL [4], DECOMP).

Generation and release of the aerosols formed under the interaction of the fuel melt and the constructional materials with concrete, are modeled in the programs VANESA and METOXDOE

The results of modeling of the SURC-4 experiment are adduced in this report. This experiment was carried out in laboratory SANDIA. The calculations were done by means of the codes CORCON and RASPLAV. The modification, which were to be done in these programs for the experiment modelling are described. On the bases of the calculation results comparison with the experimental data some new models were included into the programs. These new models allow the modelling of zirconium behavior in the metal melt in a more detailed way. Uncertainties in models and input data for modelling, which influence the results of modelling are being discussed.

Besides, calculations according to the program RASPLAV [5,6] were done in the NSI for the analysis of the processes during the melt/concrete interaction. The main attention was paid to the modelling of the melt heat balance.

2. Description of the experiment.

In this section the main characteristics of the experimental plant and the experiment conditions, described in preprint NUREG CR-1994[7], are given. The main goal of the experiment was the detailed measurement of gases generation, aerosols, and the interaction characteristics of steel-zirconium melt with concrete. 200 kg of stainless steel type 304 and 20 kg of zirconium, which was added at the quasi-steady-state of melt/concrete interaction were used as a melt. Chamber for interaction made of ceramics on the basis of MgO with the walls thickness of 10 cm, diameter 60 cm, height 110 cm was placed into the induction furnace of 280 kw. Concrete sample with the diameter of 40 cm and height 40 cm together with the heated cylinder with the weight of 200 kg (diameter 40 cm, height 20 cm). In tables 2.1 and 2.2 the weight composition of concrete and metal sample is given. In addition 6 kg of substance modelling the main products of fission, the composition of which is given in the table 2.3, were added to the metal sample until its heating up. At the quasi-steady-state of decomposition 20 kg of zirconium cylinders were added to the melt.

The experimental plant was equipped with the instruments for the analysis of the composition of the out coming gases, filters, instruments for the analysis of the aerosol composition. The duration of the experiment is about 3 hours. On the stage of preparation to the experiment, concrete and the ceramic and the ceramic chamber were equipped with a large number of thermocouples for the temperature measurement of concrete and MgO walls. The sensors in concrete were placed at an average every 2 cm on 3 radii.

The experiment SURC-4 begins at the pressure 0,8 atm and the initial temperature 325 C. The chamber of interaction together with the samples was heated in the induction furnace (power 280, kw).

In the table 2.4 the main external and internal events for

the experiment SURC-4 are given. During the experiment the unplanned power lead switching off to the work-coil took place, there were also some malfunctions of the measuring instrumentation that's why the set of experimental data is not full enough.

Alongside the main experiment the calorimetric experiments for determining the efficiency of energy input into the melt were conducted. As a result of these experiments it was ascertained, that 25+2% of power lead to the induction furnace is put into the metal cylinder. Temporal dependence of energy feed to the work-coil is given in fig.2.2. At the same time the results of the gauge experiments show the irregularity of energy feed in the cylinder volume. The fact that the concrete melting begins not in the center of the chamber, but from its side(table 2.4), testifies to it.

3. Codes, used in calculations.

In this section a brief description of the computer code CORCON and its modifications, concerning the experiment SURC-4 is given. It is necessary to mention that the modifications, made for the program CORCON from one side, were connected with the discrepancy of the code to the conditions of the experiment carry out, and from the other side, they were connected with insufficiently adequate modelling of the melt behaviour.

It is also necessary to mention that some aspects of the experiment not permit modelling in the frames of the program CORCON. First of all the question is about the heat release irregularity in metal cylinder, which can't be considered under the current code version. Besides, the experiment was carried out during approx 3 hours, and the stage of concrete decomposition took nearly an hour. The rest of the time the heating up of the cylinder and also the heating up of constructions and concrete took place. That's why the background of the concrete decomposition on the initial stage of interaction doesn't correspond to the program possibilities. Considering these aspects

the modelling of the experiment according to the program CORCON began from the time moment 5000 sec, that is to say, from the beginning of concrete decomposition.

For the program RASPLAV, which simulates thermal processes in complex systems, including phase transitions in separate components, there are no such limitations, that's why simulation was carried out from the beginning of metal heating up.

3.1. The computer code CORCON.

The program CORCON simulates the quasi-steady-state two-dimensional interaction of the steel melt with concrete (steel concrete). It is supposed, that the melt is immediately separated into two separate layers. The first layer is the layer of metals (MET). The product of concrete decomposition form the second layer - the layer of light oxides. The relative position of the layers depends on their density. CORCON assumes the existence of a thin gas film on the boundary of melt/concrete interaction. Heat transfer is determined by processes of convective and radiating heat transfer through the gas film, that is to say, for the heat flow we use expression:

$$Q = \epsilon \sigma (T_b^4 - T_d^4) + h(T_b - T_d) \Delta c \quad (1)$$

where the first term is connected with heat flows due to the radiation from the melt surface at the temperature T and from the concrete surface, heated up to the temperature of decomposition T , and the second term is connected with the processes of connective transfer through the gas film. In the model the process of heat conductivity in concrete are neglected. It is true for the developed stage of concrete decomposition, but during the experiments modelling this assumption may lead to the decrease of gas release velocity (especially water, which is separated at $T=400$ K), on the stage of metal sample heat up.

The rate of concrete decomposition is calculated from one-dimensional stationary balance of energy on the interface of the melt and concrete:

$$\frac{Q}{V} = \frac{Q}{rDH_{dc}} \quad (3)^{\wedge}$$

were V - is the volume, which will be decomposed, when energy ingresses to concrete Q kw, P - is the density of concrete, H_{dc} - is the specific enthalpy of concrete decomposition at the temperature T_{dc}

On the basis of predetermined concrete composition and the decomposition temperature T_{dc} on the data base, implemented in the program, the enthalpy of decomposition is calculated.

In the program CORCON it is also supposed, that during the melt cooling on the boundaries of interaction with concrete or atmosphere, the processes of solidification and crusts formation with the molten core existence, are possible. When the part of the layer or a full layer is solidified, the heat transfer is possible only due to heat conductivity which is much less than the heat conductivity under the convection. To simulate the process of crusts formation, some assumptions are made for the calculation of temperatures T_{sol} - "solidus" and T_{liq} - "liquidus". For the metal layer the approximation of three phase diagram for iron-chromium-nickel alloy is used. The influence of other metals on T_{sol} T_{liq} is neglected. For the oxide layer the pseudo binary diagram is used in which uranium and oxides form the first component and concrete form the second component. For these two components it is supposed that they form an ideal solution both in liquid and solid state.

In the program CORCON it is supposed that chemical reactions process so that to provide equilibrium of concentration, determined by minimum of a free Gibbs theory for 38 chemical components, formed by elements. All 38 components, considered in the program CORCON, are given in the table 3.1.

3.1.1. Program CORCON modification

The code modifications were done, because the program CORCON doesn't allow to simulate experiment SURC-4. In particular, as it was already mentioned the program is developed for the

two-dimensional modeling of concrete decomposition, and the experiment SURC-4 is one-dimensional. For the account of this aspect some changes were made in subprogram SURFEB, which exclude radial melting of the side walls of the experimental chamber.

According to the conditions of the experiment an additional program was done. This program allows to simulate zirconium addition according to the experiment script.

The time dependence of the heat source power, put into the melt was also realized.

The account of energy loss through the ceramics side walls was done by decreasing of heat input into the melt layer. The loss value varied in the calculations. As a loss value, the results of the calculations up to the program RASPLAV were used.

3.2. The program RASPLAV

The program RASPLAV is determined for two-dimensional modelling of heat conductivity process in the systems with complex geometry with various heat release sources. The main physical processes, simulated in this complex of programs are the following:

- Phase transitions (melting and vaporization);

Simulation of phase transitions is done by assigning thermal dependences of thermophysical characteristics: heat capacity C and heat conductivity k . Convective mixing in the melt with temperature higher than the melting point is simulated by increasing the coefficient of heat conductivity up to value $k=5-10$ w/cm K.

- Movement of the fuel elements through the melt and also movement of the concrete decomposition products;

- Realization of various variants of boundary conditions on the outer surfaces and on the inner boundaries for simulating various conditions of the materials cooling from the boundary;

- The program admits stratification of the melt into layers with the possibility of assigning heat transfer coefficients between the layers;

- In the program the models of chemical reactions are also realized, these include reactions between melted metals and gases, formed during concrete decomposition.

The solution of a full heat conductivity problem in two-dimensional geometry, allows to make a detailed modelling of processes, concerning formation and repeated melting of the crusts, formed near the boundary of the melt with cooling media.

So, in contrast to program CORCON the program RASPLAV allows to calculate transitional processes and also, the developed stage of interaction with concrete with the account of real geometry of the experiment, and various constructional materials, characterized by their own set of thermophysical constants.

In the calculations, given bellow, it was assumed that the melt consisted of two layers - metal layer and oxide layer.

4. Modelling results according to the program CORCON

4.1. The preliminary modelling of the experiment

The initial data for preliminary calculations are given in the table 4.1. At this stage of investigations the variations of some input parameters were made - power input into the melt (the account of side losses into ceramics), the initial temperature of the melt, the environment temperature. Two values 62 and 45 kw for the source power were used. The first variant corresponds to the absence of the energy losses through the ceramic wall. The 17 kw losses for the second variant, correspond to the estimation of the side losses up to the program RASPLAV

As an initial temperature of the melt, for the first variant, the experimental value of the temperature to the time moment of 6300 sec, which is equal to 1750 K was chosen. But at this temperature in the program the metal layer remains solid. The alloy melting temperature, calculated in the program, is 1780 K.

In picture 4.1 the dependence of the melt temperature from time for the initial temperature 1750 K is given. The whole power feed to the melt, in this case, goes to heating up and melting of steel, that's why temperature doesn't practically change in the course of time. In order to avoid contradictions with the experiment, we chose the initial temperature, which was higher than the temperature of steel melting.

In fig.4.2 the time behaviour of the melt temperature for variants 2 and 3 is given. The addition of cold zirconium up to 7140 sec leads to a sharp temperature decrease, which gradually increases up to the initial value due to the source of energy and heat, released during zirconium oxidation. The total power of the chemical heat is about 15 kw. After the energy source switch off to 7446 sec, the chemical heat release is insufficient to maintain temperature at the previous level and the temperature falls until the second switch of the energy source. The temperature increases slowly until the end of the experiment.

The depth of melting, shown in fig.4.3, coincides sufficiently with the experimental values. Quantitative data, concerning the time behaviour of zirconium is absent, in fig.4.4 the results of modelling are given. As a result of zirconium oxidation, its mass decreases constantly and in the end of the experiment it is about 5-7 kg.

4.2. Comparison the modelling results with the experiment

4.2.1. The temperature of the melt

The comparison of calculation and experimental data, given in fig. 4.2, depicts some discrepancies in the time behaviour of the melt temperature. Firstly, after zirconium addition the temperature in the experiment grows very quickly. The characteristic rate of heating is about 0.43 cal/sec. Estimation of the heat source power, necessary for heating, in neglecting possible energy losses gives:

$$Q = mTc \quad 70 \text{ kW}$$

where m is mass of melt, kg;

c - specific heat capacity of the melt, J /kg/ cal;

T - the rate of heating, pal/sec.

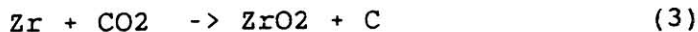
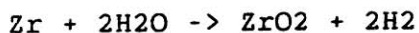
As it was already mentioned, chemical heat release is only 15 kw, what is obviously insufficient for mining such rate of heating and in the experiment, significantly more intensive energy release during chemical reactions is observed.

Secondly, after the repeated switch of the heat source, the growth of the temperature was not observed in the experiment. It may be connected with the fact, that by the time of 8706 sec there was no zirconium in the melt.

So, the observed temperature behaviour, apparently, is connected with the models incompleteness of chemical reactions with zirconium.

4.2.2. Zr behaviour

The chemical analysis of the metal alloy composition after the experiment showed the absence of metal Zr in the melt. The simple estimate shows, that in the frames of chemical reactions using codes CORCON, we failed to oxidize Zr fully. From the results of the experiment we can see, that the volume of the decomposed concrete is about $2.7 \times 10^4 \text{ sm}^3$. As far as basaltic concrete contains 5% H₂O and 2.5% CO₂, it not difficult to calculate, that a full amount of water, separated in the course of concrete decomposition, is about 180mol and a full amount of CO₂ - 40 mol. The amount of zirconium added to the melt - 20 kg (220 mol). In the model of chemical reactions CORCON the following reactions are taken into account:



that is to say, to oxidize 1 mole Zr, 2 moles of H₂O and 1 mole CO₂ are used (if it is a reaction with coking effect). That's why, it is possible to oxidize no more than a half of zirconium in the result of these reactions.

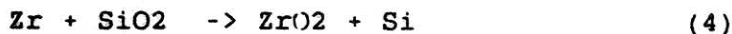
That's why the comparison of the melt temperature behaviour

shows, that the model of chemical reactions CORDON is not full, so we searched for the chemical components, which could have explained the melt behaviour in the experiment.

4.3. The change of the chemical reactions models

As additional chemical reactions, the exothermal reactions of Zr oxidation by the products of concrete decomposition in condensed phase may take place. The analysis of the melt components, shows that one of the reagents may be SiO₂, which constitutes the main part (55%) of the concrete decomposition products. It follows from the fact, that in the course of this reaction the heat release may be 200 kw/mol Zr, that is in terms of entrance rate of silicon oxide to the melt makes up approx 60-70 kw. In this case the time of zirconium oxidation will be significantly reduced and by the end of the calculation, there will be Zr in the melt.

As for all other components, we assumed, that the rate of the reaction



is limited by SiO₂ entrance. The result the reaction is accounted in the mass and heat of metal and oxide layers balance. Thermophysical data, concerning Si were taken from the reference book.

4.4. The results of the calculation according to the modified CORCON version

In this section the comparison of calculation results with the published experimental data is given. The data were taken from the work [7].

The initial data of the calculation are given in the table 6.1. As an ambient temperature the 1400 and 1700 K were chosen. These are the maximum values for the ambient temperature, observed in the experiment.

In fig.4.5. the plot of the melt metal layer temperature

dependence on time for two variants of calculation is given. In this very picture the plot of time dependence of the heat source, put into the melt in arbitrary units is given also. After the addition of 20 kg of Zr for 7140 sec, the melt begins to warm up under the action of total heat of the chemical reactions and the source. The temperature curve has a max slope for variant 2, which coincides with the experimental rate of heating. The heat source is switched off for 7446 sec, the melt is heated up due to the heat of the chemical reactions what is seen from the change of the temperature curve slope. On 7902 sec. the repeated switch on of the heat source takes place. For the second variant by this moment we can observe practically full Zr burn-out (fig.4.6). For the first variant, significantly larger value of energy losses with radiation regulates the temperature growth after the source is switched off Zr burning lasts longer and ends by 8300 sec. Then the melt begins to cool down slowly. The last change of the temperature curve slope is connected with the heat source switch off for 9750 sec.

From fig.4.5. we can see qualitative agreement between the experimental results and the calculations according to the modified model CORCON. In fig.4.7 the time dependence of the concrete melting depth for two variants is given. From the plot we can see that after the addition of Zr to the melt the rate of melting increases. The average calculated melting rate changes from 12-13 cm/h before Zr addition and to 30.5-32.5 cm/h after Zr addition. Experimental results are in the interval between the calculated results for these two variants. In fig. 4.8 there is a plot of the melt's energy source and flows dependences on time for variant 1 - chemical heat release Q_{react} , energy losses for concrete decomposition Q_{abl} and energy losses with radiation Q_{atm} . There are no experimental data, concerning these values. Calculated results depend on selection of a concrete decomposition temperature and on the ambient temperature. The time of changing the slope of curves correlates with time of addition and full oxidation of Zr, switching off the heat source.

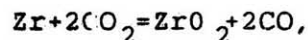
As far as there is no Zr in the melt, the endothermic reaction of chromium oxidation with heat absorption on the level of 0.7 kw is going on. After the addition of the Zr the total heat release

changes up to 60-80 kw. After Zr has oxidized fully, during a short time the endothermic reaction of pure carbon oxidation with heat absorption on the level of 25 kw proceeds in the melt. After the full carbon oxidation, the oxidation of chromium with the heat absorption which doesn't excess over 1 kw is going on. Let's notice, that the calculated heat release as a result of the chemical reactions includes the work, concerning carrying of the reaction products from metal layer to the oxide layer.

In fig.4.9-4.12 there are plots of gases release dependences-products of the concrete decomposition on time. The calculated gas temperature is close to the melt temperature. It is seen from the calculations, that after Zr addition into the melt, the consumption of H_2 , H_2O and CO_2 increases. At the same time the consumption of CO decreases approx by a factor of 10^3 , because of the "coking" reaction, when CO_2 is reduced to pure carbon. After the full Zr oxidation, the pure carbon oxidizes to CO and its consumption grows again.

The calculated H_2 Consumption coincides with the results of the experiment in the best way. It is bound up with the fact, that during the reactions with water vapour the oxidation of one of the metals takes place, there are no other reactions with water vapour.

And the experiment demonstrates this fact. As far as the difference in more than two orders for CO is concerned, it is conditioned by the fact, that in the model of chemical reactions CORCON only the second reaction out of (3) is concerned for the channels of metals oxidation by CO_2 . Alongside with this channel there is also a channel



which is not taken into account in the program.

4.5. Models uncertainty

4.5.1. Uncertainties of the input data

As it was mentioned above, in the model CORCON the calculation T_{sol} and T_{liq} is done using a triple phase diagram Fe-Cr-Ni. The preliminary calculation showed, that T_{liq} of the metal layer is higher than 1746 K. While the experimental results show, that at 1746 K the sample is melted. The lack of coincidence between calculations and the experiment is the result of the fact, that the model of determining T_{sol} and T_{liq} doesn't consider real chemical composition of steel, the existence of ceramic MgO and etc.

In the calculations we assumed, that the side losses of heat are constant, there were accounted by reducing the heat, put into the melt by 15-20 kw. Heat conductivity to concrete and atmosphere is modelling from the expression (I), in which the first term is the radiation component and the second term is the convective component. The temperature of various concrete decomposition T_{dc} which enters into the equation of thermal losses into concrete and T_{sur} which enters into the equation of thermal losses into the atmosphere are the key parameters. They determine the total heat balance and influence the rate of concrete erosion. So, the analysis of the model sensibility to T_{sur} showed, that the fraction of heat, carried away with the radiation from the melt surface to the atmosphere may constitute from 30% to 80% of the heat put into the melt. Today, there are no reliable models or data, allowing to choose T_{dc} and T_{sur} . The question of correct choice is still opened.

4.5.2. Uncertainties of the chemical reactions models

In the model of chemical reactions of the code CORCON the equilibrium thermodynamic approach to the chemical interaction is realized. As far as the products of concrete decomposition with Zr are concerned, it is necessary to take into account the kinetic character of interaction. In calculations the rate of the reaction between Zr and SiO_2 was limited by SiO_2 entrance from concrete. But by the moment of Zr addition, there was already some amount of SiO_2 in the melt (about 70 moles). That's why, the question if interaction kinetics of various components of the melt is very important. The rate of such reactions may change in wide range. Besides, it is not clear, where such interaction may take place, -

on the layers contact surface, in the volume and etc.

This and other kinetic processes could influence significantly the melt's temperature, Zr behaviour, release of gases. The main difficulty realization of the kinetic approach to the chemical interaction is the absence of data, concerning the kinetics of this reaction.

5. Experiments modelling up to the program RASPLAV

The experiment SURC-4 modelling was done using the program complex RASPLAV. In such calculations we tried to simulate the whole time script of the experiment.

Because of the fact, that the program HFCGKFD allows to calculate not only quasi-stead interaction, but also transitive processes in various medium, the comparison with the experiment was done not only by the rate of melting, but also by the thermocouples readings, maintained into various materials - steel, ceramics, concrete. All these allowed to determine energy losses under the interaction.

For specification of initial data, concerning thermophysical constants and also the initial data of the experiment the simulation of the calibration tests was done.

5.1. Calculation of experiment

For specification of thermophysical constants of the materials and also, the conditions of the experiments, the calculations of the calibration experiments described in [7] were done before hand. The most important parameter, which can significantly influence the rate of sample heating up is the distribution of the heat sources in the metal cylinder volume. In the experiment the steel cylinder had a thermal insulation made of a special isolator, that's why we calculated fully thermally insulated problem with the zero flows on the boundaries.

From the thermophysical constants for the metal cylinder in

[7] only experimental data, concerning steel heat capacity, used in the experiment were placed. In the course of modelling the estimations of heat conductivity in metal were done.

Modelling of the calorimetric test was done in two stages. On the first stage the steel heat conductivity was crudely estimated, using the time of temperature outcome to the balanced value. Three values of the inductor power were used in the test - 100, 175, 250 kw. After the source and the transition processes switch off, the temperature equilibrium was established. The time of heating up and, consequently, the temperature gradients in these three cases differed greatly. According to the modelling results of levelling the temperature, the steel heat conductivity made up 0,15 wt/cm K. Strong nonuniformity of heating (the outer areas of the cylinder heated up more than the inner ones) was conditioned by nonuniformity of the energy input into the steel cylinder. That's why, on the second stage the distribution of heat release on radius was determined. It the result of calculations, it was determined, that the heat release power on the brim of the cylinder is more than ten times the heat release in the center of it. In all cases, it was considered, that approximately 25% of the feed power is released in metal. The time and the equilibrium temperature coincide quit well with the experimental ones.

For modelling of the radial distribution the heat release profile was preset in the form of

$$q = q_0(1+10(r/a)^2) \quad (5)$$

In fig.5.2 the calculations and experimental values of temperature in various radial points with such choice of heat release is given. From the picture we can see, that the use of the formula (5) is described by the calorimetric test sufficiently good. The same calculations were done for all three experiments. In all cases the satisfactory agreement with the experiment is observed.

The found distribution of the heat sources was used in the experiment calculations.

5.2. Interaction modelling results up to the program HFCGKFD

For modelling experiments SURC-4 the script was chosen. This script includes not only the stage of developed interaction of the metal melt with concrete, but, also, the modelling of the stage of heating up and melting of the metal cylinder was done. The time script of the calculation is given in table 2.4. The distribution of the heat source in the metal layer was chosen in accordance with the results of calorimetric tests modelling using the formula (5).

5.2.1. Thermophysical constants.

For modelling the processes of heat conductivity in the melt, it is necessary to preset thermal dependences of the heat conductivity coefficient k and heat capacity for all materials, used in the experiment.

Ceramics on the basis of MgO. In order to study thermophysical characteristics of ceramics in [7] special experiments were conducted. The following values for MgO were offered:

density $\rho_{\text{MgO}} = 278 \text{ g/cm}^3$

heat capacity $C_{\text{MgO}} = 1.25 \text{ /g}$ (mean value)

heat conductivity $\min (-5 \cdot 10^{-5} T + 0.082, 0.020) \text{ (w/cm K)}$

In table 5.1 numerical data of the temperature dependence of heat capacity and heat conductivity of ceramics up to the temperature 1200°C are given.

Steel. For the cylinder made of steel mark 304 the data, concerning heat capacity are given in the report [7] and in the table 5.2. Heat conductivity coefficient was selected as being independent from the temperature, in accordance with the results of calorimetric tests modelling.

Concrete. For the concrete composition, given in the table

2.2, the calculations of its thermophysical characteristics, with using the corresponding sub-programs of the program CORCON, were done. The melting point T_{liq} and the temperature of solidification T_{sol} were preset in accordance with [3]. Thermogram for basaltic concrete, used in this experiment shows, that during concrete decomposition, approximately 1.5 weight percents of CO_2 and about 5% of water vapours are released. Free water vaporizes in the range 50-100⁰C and the bound water in the range 400-750⁰C and at the temperature of 700⁰C decomposition of $CaCO_3$ and CO_2 release take place. The concrete decomposition temperature for the program CORCON was 1500 K. There are no data on concrete heat conductivity in [7] and its value was chosen according to the work [8] and it varied in the calculations in the range 0.01-0.02 wt/cm K.

The used data are given in the table 5.2.

5.2.2. Stage of the melt heating up.

The goal of modelling the initial stage of interaction was the choice of heat release mechanisms on the contact boundaries of the media: metal-concrete, metal-ceramics.

The comparison of calculations data with the experimental readings of thermocouples maintained into the steel cylinder, ceramics and concrete, allows to make conclusions, concerning thermal losses through the side surface, contacting with ceramics and the bottom boundary with concrete. In fig.5.3 the calculated and experimental values of the steel cylinder temperature in the point $h=5$ cm and $r=18$ cm are given. The calculated values of the temperature are slightly lower, this is connected with large losses into ceramics and concrete in comparison with the experiment. It is also pointed out by the curves in fig. 5.4, which demonstrate the time behaviour of thermocouples readings, put into ceramics approx at a distance of 10 cm from the bottom boundary of the steel cylinder. Large values of temperature are received for thermocouples reading in concrete on various depth (0, -1 and -3 cm) (fig.5.5.).

The cause of such difference may be undiffisional mechanisms of heat transfer on the contact boundaries in the result of incomplete and in compact contact of the adjoining planes. As we

can see from the drownings qualitatively the picture corresponds to the observed one in the experiment, but the time of beginning and end of steel melting somewhat longer, than the time observed in the experiment.

5.2.3. Stage of developed interaction

On the stage of developed interaction after full melting of the steel cylinder, we may consider, that the heat transfer to the ceramics wall will be diffusional. That's why, after melting, the heat conductivity model was used. At the same time, it was assumed that there was no gas film on the boundary with ceramics.

The existing version of the code RASPLAV doesn't allow us to calculate chemical reactions between the components, that's why, Zr addition to the melt wasn't done and the increase of heat release in the result of chemical reactions wasn't taken into account. In fig. 5.6 there is a dependence of the concrete decomposition depth on time, calculated up to the program HFCGKFD. The process decomposition begins at the time moment 6000 sec, what approximately corresponds to the experiment. The rate of decomposition, while the melt front moves along the heated up concrete, corresponds to the experiment. Later on the rate, somehow, becomes slower. At the same time, the average temperature of the melt is 1750 K, what is close to the experimental values.

In the fig. 5.7 the calculation results of heat losses with radiation from the above boundary of the melt and the losses on the contact boundary of the melt with the side surface of ceramic walls are given. It follows from this that the schedules, that on the developed stage, about 20 kw out of input 62 kw release from the melt surface with the radiation. The losses through the side surface of ceramics on the developed stage of the experiment grow nearly linearly and are 5 to 10 kw. So, from the calculations, using code HFCGKFD, it follows from this that full losses make up about 50% of the input energy.

So, while modelling the experiment SURC-4 up to the program HFCGKFD, we managed to co-ordinate the results of modelling the melt heat balance, that comes from the agreement between measured

and calculated temperature. But some differences are connected with the overestimation of heat flows to ceramics and radiation losses.

6. Summary

The goal of this work is the SURC-4 experiment modelling. This experiment was carried out in laboratory SANDIA USA, with the help of codes CORCON and HFCGKPD. In this report we tried to simulate first of all, the heat balance of the melt. It follows from the results of the experiment that:

1. For proper modelling of the thermal regime, it is necessary to include some new models, such as a model of radiation exchange of energy between the melt and concrete. It is necessary to include these models into the program CORCON and into the program HFCGKPD also. This will allow us to exclude some of the uncertainties, connected with assigning of input data.

2. During the work with the program CORCON it became clear, that the model of chemical reactions is not full. Inclusion of an additional reaction of Zr oxidation by the products of concrete decomposition in oxide phase (SiO_2), have led to the qualitative coincidence of the calculated results of temperature, behaviour with experimental data. Besides, it was discovered, that some of the reactions proceed in other channels (reaction of Zr oxidation by CO_2). At the same time, the question, concerning kinetics of the chemical reactions at the condensed phase, is still not clear.

3. Further investigations concerning the formation of the data basis on thermophysical properties of the materials in particular concrete, metals melt and oxides are necessary. Even in a relatively simple case of a three component phase diagram Fe-Cr-Ni, the measured values of the melting temperature turned out to be lower calculated ones.

References

1. J.E.Brockmann. Ex-vessel aerosol source terms in reactor accidents. Progress in Nuclear Energy. V.19, No.1, pp.7-68, 1987.
2. M.Corradini, H.H.Reineke. A review of the BETA Experimental Results and Code Comparison Calculations. Nuclear Science and Engineering. V.102, No.7, pp.260-282, 1989.
3. Cole R.K., Kelly D.P., Ellis M.A. CORCON-MOD2: A Computer Program for Analysis of Molten-core Concrete Interactions. NUREG/CR-3920, SAND84-1246, 1984.
4. M.Reinmann, S.Stiefel. The WECHSL-Mod2 Code: A Computer Program for the Interaction of a Core Melt with Concrete including the Long Term Behaviour. KfK 4477, 1989.
5. Р.В.Арутюнян, Л.А.Большов, и др. Численное моделирование нагрева, плавления и испарения металлов при импульсно-периодическом лазерном воздействии. Препринт ИАЭ-4121/16 М., 1985.
6. Р.В.Арутюнян, Л.А.Большов, и др. Моделирование проплавления корпуса реактора и опускания топлива в бетоне при тяжелых авариях на АЭС ВВЭР с помощью комплекса программ расплав. Препринт ИАЭ им. И.В.Курчатова 4778/3, 1989.
7. E.R.Copus, R.E.Blöse, J.E.Brockmann et.al. Core-Concrete Interactions Using Molten Steel with Zirconium on a Basaltic Basemate: The SURC-4 Experiment. NUREG/CR-4994, 1989.

Table.2.1.

Chemical Composition of Basaltic Concrete of test SURC-4

	Oxide	Weight %
14	Fe ₂ O ₃	6.3
	TiO ₂	1.1
	K ₂ O	5.4
	Na ₂ O	1.8
9	CaO	8.8
13	MgO	6.2
10	SiO ₂	55.2
11	Al ₂ O ₃	8.3
↖	CO ₂	2.5
↗	H ₂ O	4.2
	SO ₂	0.2
		<hr/> 100.0

Table 2.2.

Chemical Composition of Steel of test SURC-4

Element	Weight %
Fe	71.18
Cr	18.50
Ni	8.25
Si	0.50
Cu	0.25
Mo	0.25
Mn	1.0
C	0.04
P	0.02
S	0.01
	<hr/>
	100.00

Table 2.3

Chemical Components added to the metal model for
modelling fission product

Component	Quantity (kg)	Category
Molibdenum (Mo)	2.0	
Tellurium (Te)	0.5	Chalcogenes
Lanthanum Oxide (La_2O_3)	1.17	Trivalentes
Cerium Oxide (CeO_2)	1.23	Tetravalents
Barium Oxide (BaO)	1.10	Alkaline Earths

Table 2.4

Events of test SURC-4

Time (min)	Time (sec)	Event
0.0	0.0	Start of data acquisition system
10.7	642.0	Power supply on power meter reading 98 kw
44.0	2640.0	Power increased to 200 kw (power meter)
80.5	4030.0	Power increased to 245 kw (power meter)
104.3	6258.0	Thermocouple C ₄₁ failed (r=18.0 cm, z=0.0 cm)
105.4*	6324.0	Thermocouple C ₁ failed (r=0.0 cm, z=0.0 cm)
111.9	6714.0	Thermocouple C ₂₁ failed (r=10.0 cm, z=0.0 cm)
119.0	7140.0	Zirconium metal delivered to the melt (20 kg)
124.1	7446.0	Power supply off
131.7	7902.0	Power supply off (245 kw)
144.8	8688.0	Power supply off
145.1	8706.0	Power supply off (245 kw)
162.5	9750.0	Power supply off
177.6	10656.0	Data acquisition system terminated

This moment is taken to be the onset of the interaction with the concrete.

Table 3.1

Chemical Components Considered by the program CORCON

Oxide	Metal	Gas	
FeO	Fe	C(g)	NH ₃
MnO	Cr	CH ₄	N ₂
ZrO	Ni	CO	O
Cr ₂ O ₃	Zr	CO ₂	O ₂
NiO	Mn	C ₂ H ₂	OH
* FPMO ₃	C	C ₂ H ₄	CHO
Fe ₃ O ₄	* FPM	C ₂ H ₆	CH ₂ O
Mn ₃ O ₄	** X	H	CrO ₃ (g)
		H ₂ O	FPMO ₂ (g)
		N	FPMO ₃ (g)

* Pseudo-components representing four groups of the fission product

** Inert components considered as element X in the equilibrium calculation

Table 4.1

The initial data for preliminary calculations

	Var.1	Var.2	Var.3
1. Source power, kw	45	62	45
2. Initial temperature of the melt, K	1746	1795	1795
3. Environment temperature, K	1400	1700	1700
4. Temperature of the concrete decomposition, K	1550	1550	1550
5. Radiosity of the environment	0.8	0.8	0.8

Table 4.1

The initial data for calculation

	Var.4	Var.5
1. Source power, kw	45	45
2. Initial temperature of the melt, K	1795	1795
3. Environment temperature, K	1400	1700
4. Temperature of the concrete decomposition, K	1550	1550
5. Radiosity of the environment	0.8	0.8

Table 5.1

Temperature dependence of Specific Heat and Conductivity
Coefficient of ceramics

Temperature (C)	Specific Heat (ws/gm K)	Conductivity (w/cm K)
22.0	0.885	0.08009
100.0	1.018	0.08082
200.0	1.123	0.07544
300.0	1.184	0.06869
400.0	1.211	0.06018
500.0	1.242	0.05379
600.0	1.268	0.04365
700.0	1.285	0.04281
800.0	1.300	0.03898
900.0	1.307	0.03665
1000.0	1.314	0.03465
1100.0	1.325	0.03347
1200.0	1.330	0.03249

Table 5.2

Specific Heat of Steel and Concrete used in test SURC-4

Temperature (C)	Specific Heat ⁽¹⁾ (ws/gm K)	Specific Heat of Concrete ⁽²⁾ (ws/gm K)
300	0.5100	0.7590
400	0.5234	0.9479
500	0.5368	1.0415
600	0.5502	1.0973
700	0.5640	1.1353
800	0.5774	1.1638
900	0.5908	1.1866
1000	0.6042	1.2058
1100	0.6176	1.2227
1200	0.6314	1.2367
1300	0.6448	1.2481
1400	0.6581	1.2449
1500	0.6715	1.2546
1600	0.6853	1.2650
1700	0.6987	
1700-3000	0.7950	

(1) Data obtained from [7]

(2) Calculated data from CORCON

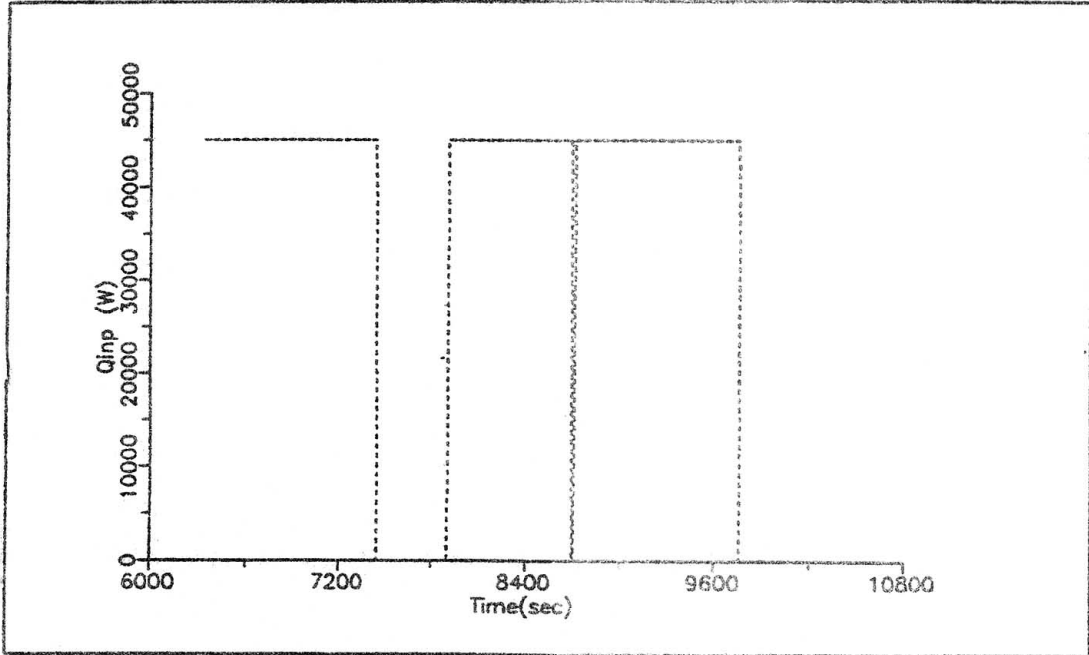


Fig.2.1. Time dependence of power input into the melt

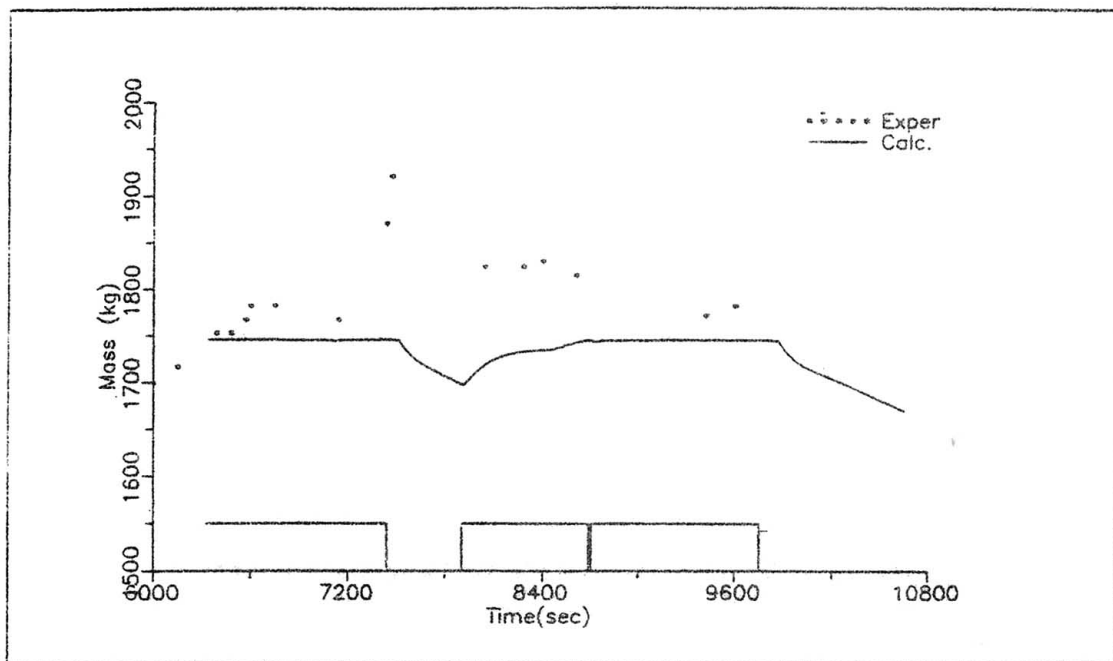


Fig.4.1. Time dependence of the melt temperature for variant 1

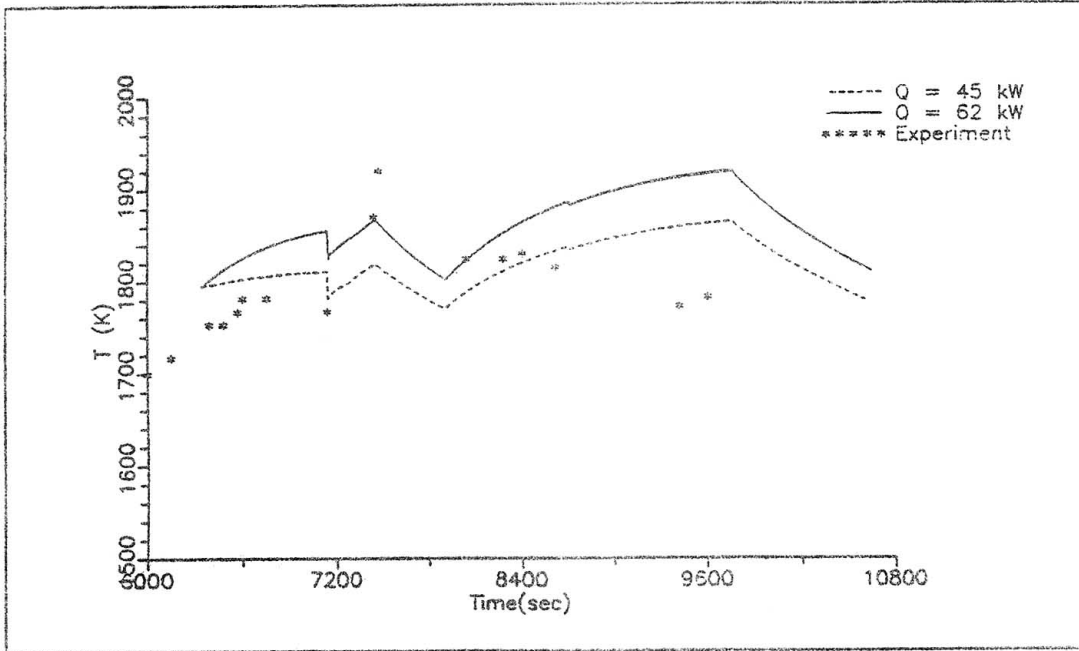


Fig.4.2. Time dependence of the melt temperature for variants 2 and 3

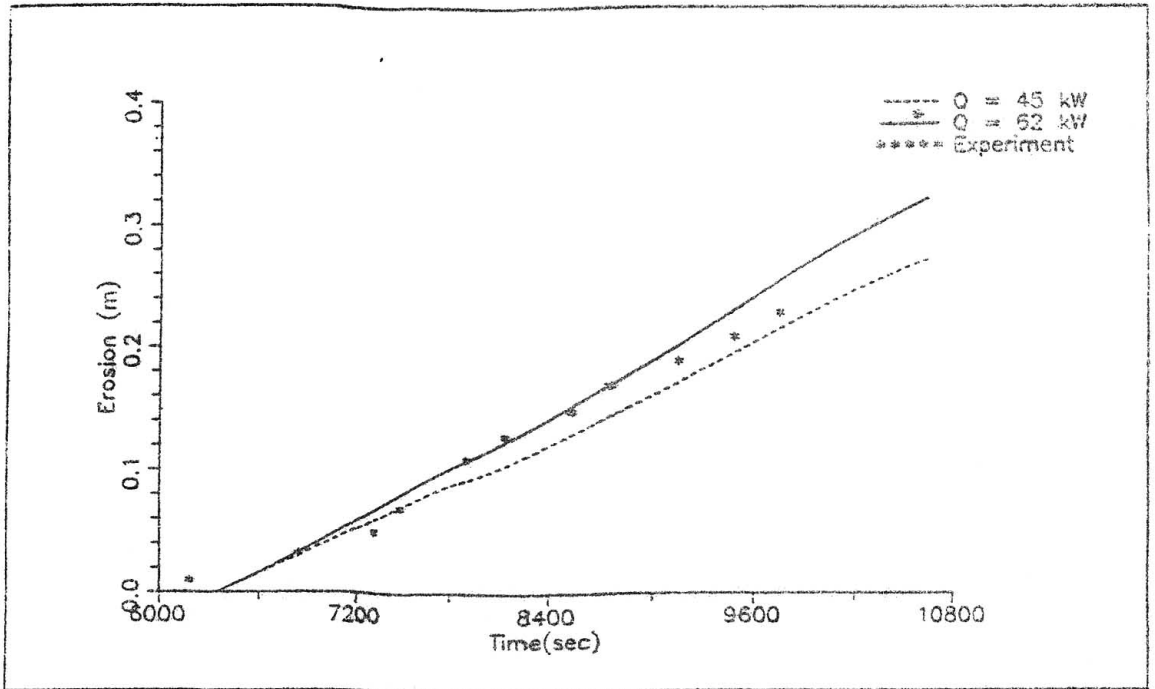


Fig.4.3. Time dependence of the concrete erosion for variants 2 and 3

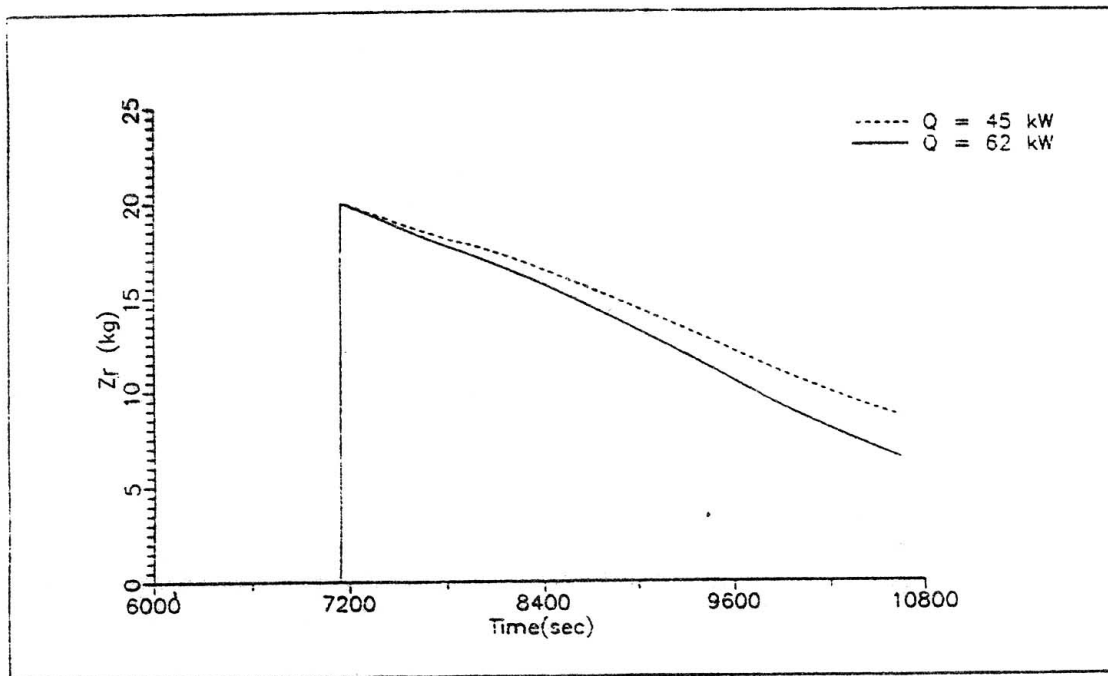


Fig.4.4. Time dependence of zirconium mass for variant 2 and 3

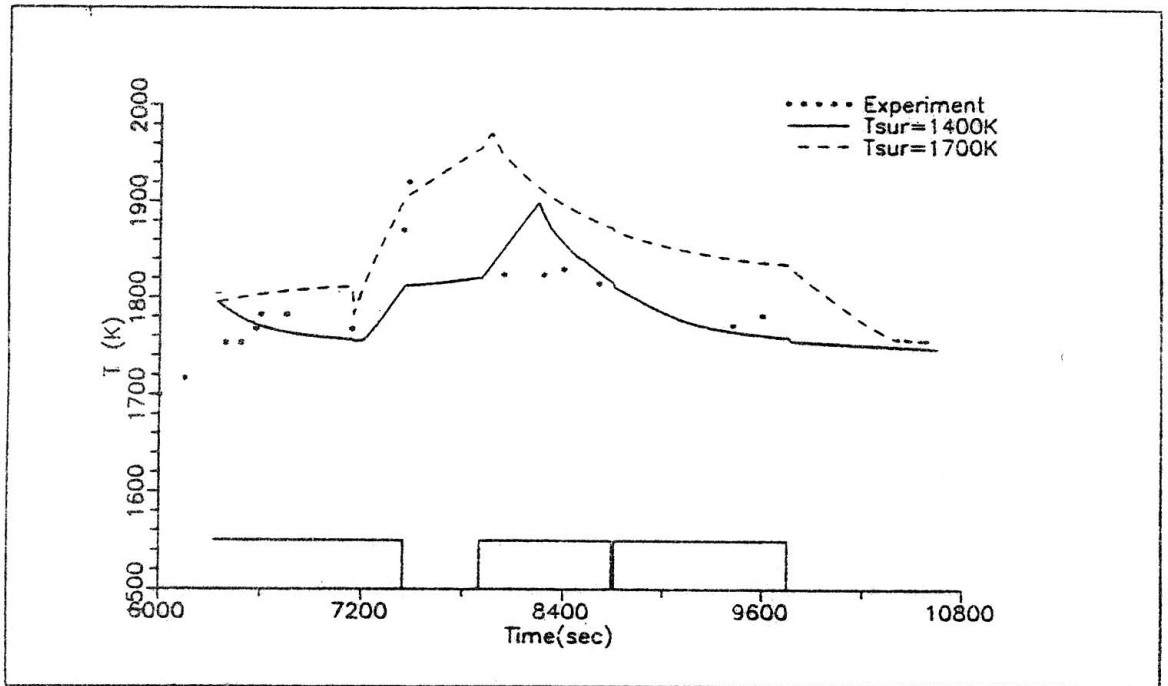


Fig.4.5.

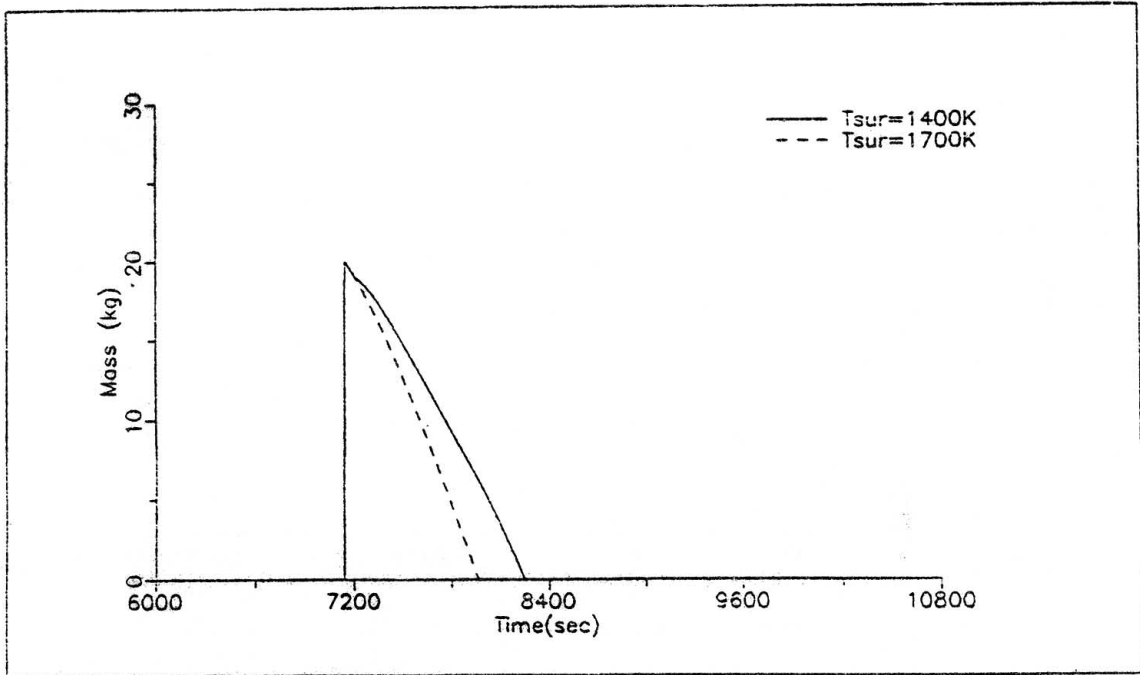


Fig.4.6. The change of Zr mass during time for variants 4 and 5 (with account of the reaction of Zr with SiO_2)

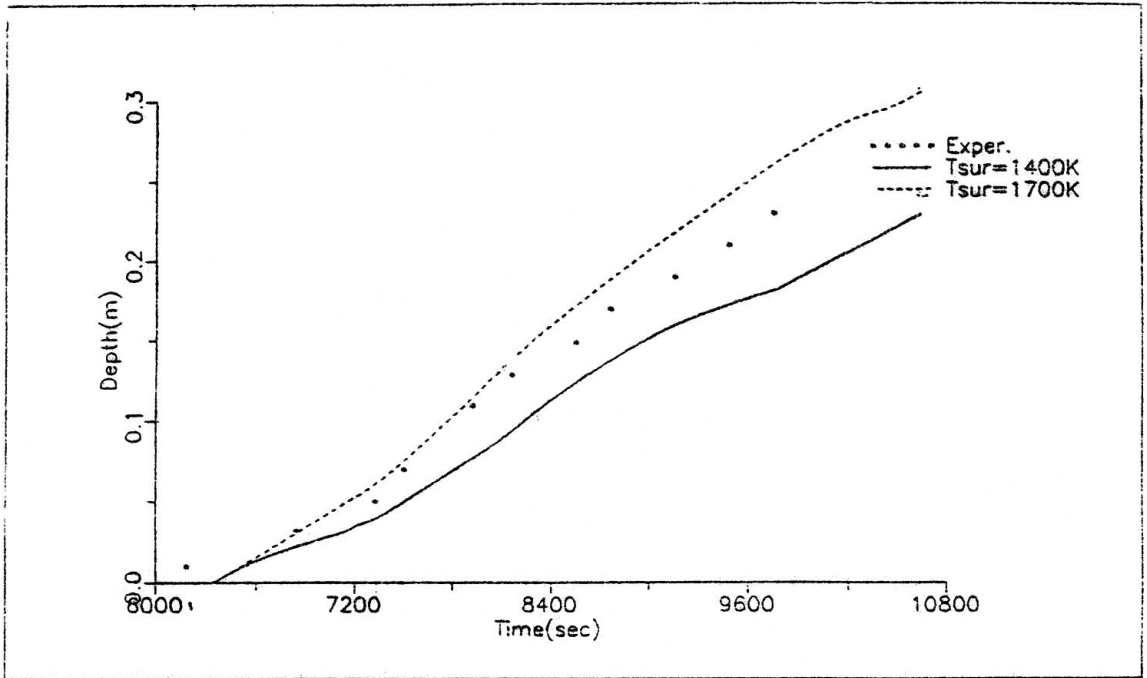


Fig.4.7. Time dependence of the concrete erosion for variants 4 and 5 (with account of the reaction of Zr with SiO_2)

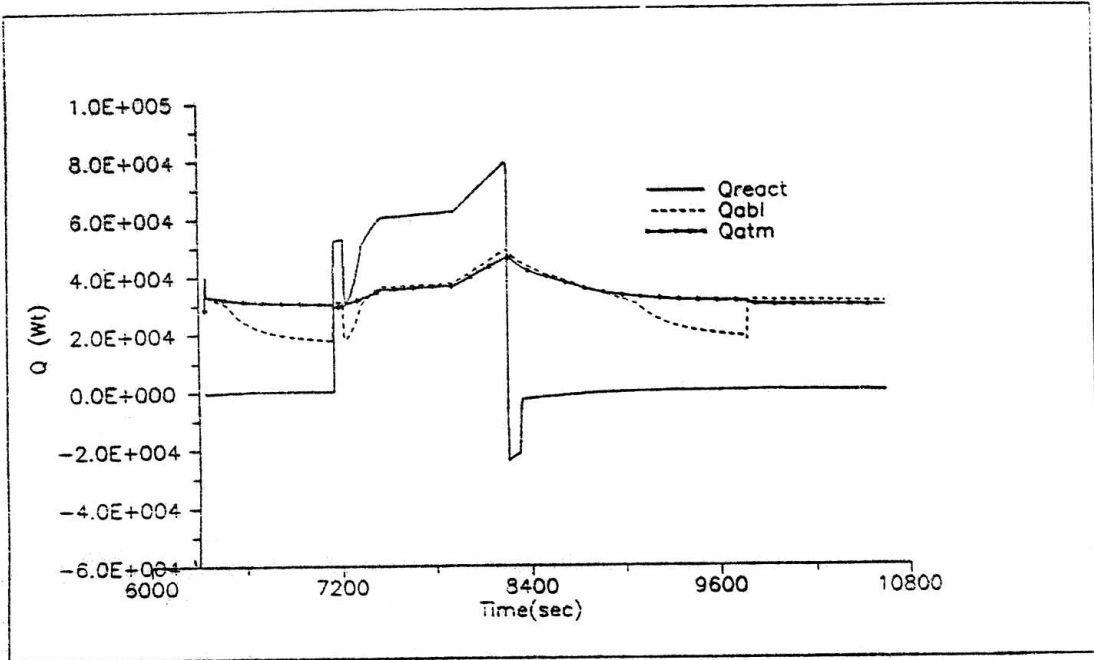


Fig.4.8. Time behaviour of heat sources and flows for the variant 4 (with the account of Zr reaction with SiO₂)

- Q_{react} - chemical heat release
- Q_{abl} - energy, going to concrete decomposition
- Q_{atm} - radiation energy losses

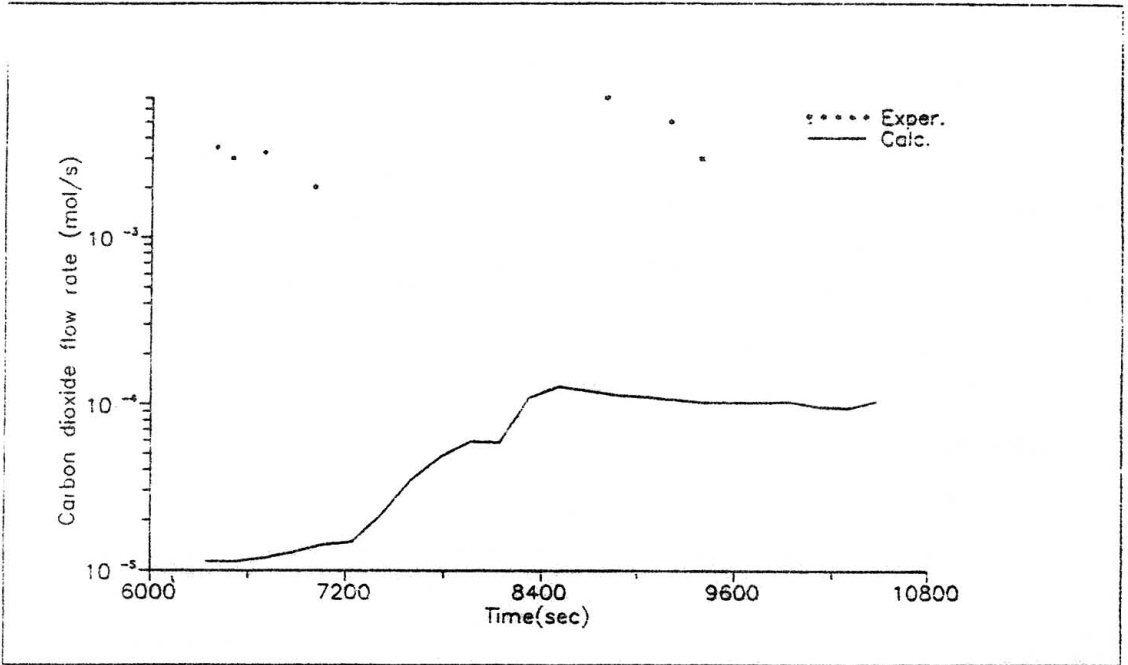


Fig.4.9. Time dependence of CO₂ generation rate for variant 4

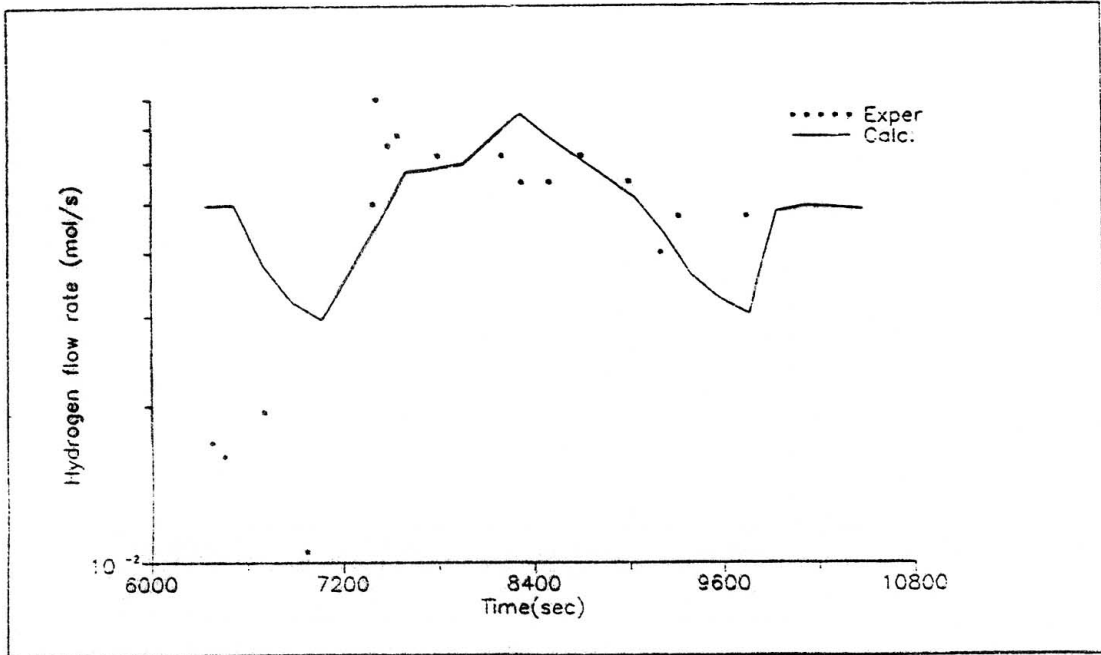


Fig.4.10. Time dependence of H_2 generation rate for variant 4

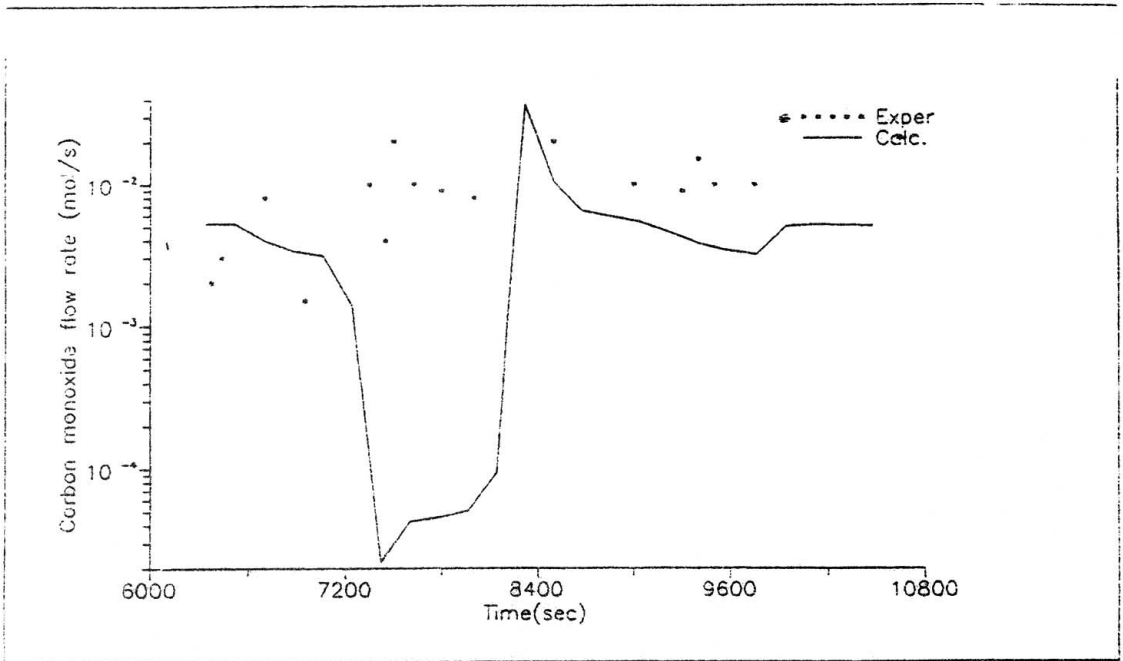


Fig.4.11. Time dependence of CO generation for variant 4

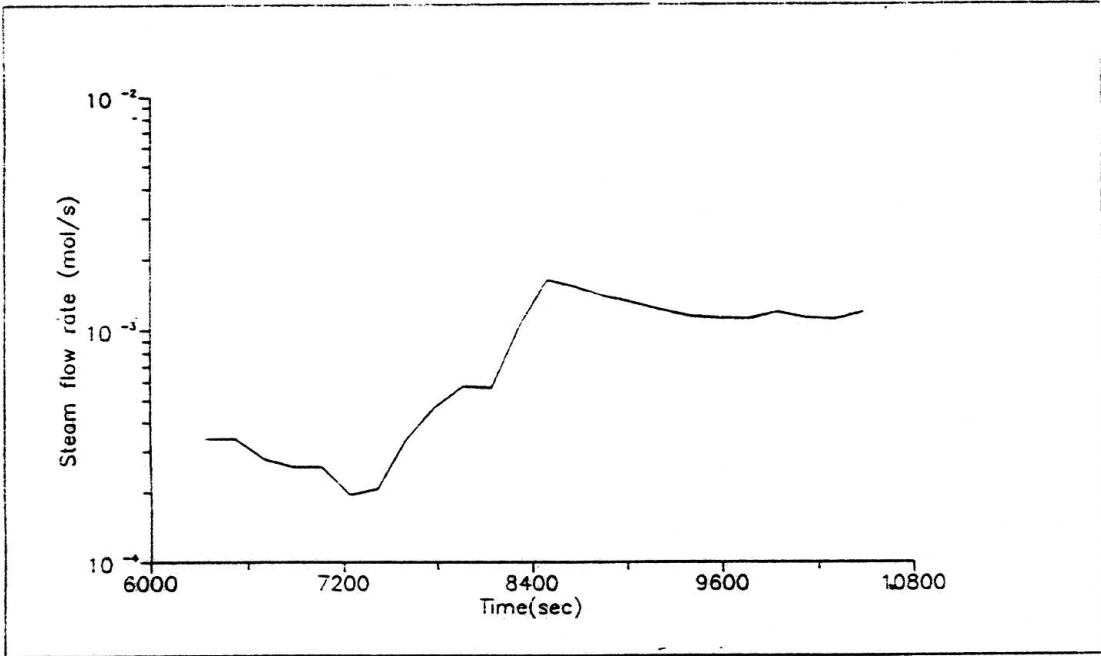


Fig.4.12. Time dependence of H_2O generation rate for variant 4

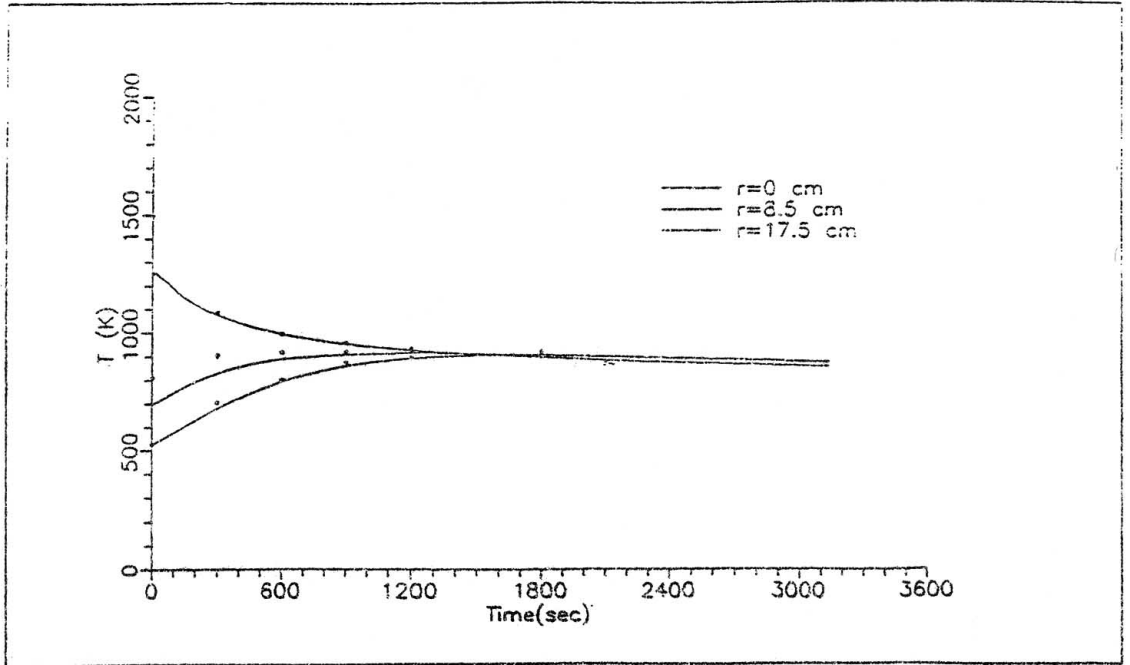


Fig.5.1. Comparison of the calculation results, concerning the temperature leveling for the calibration experiment

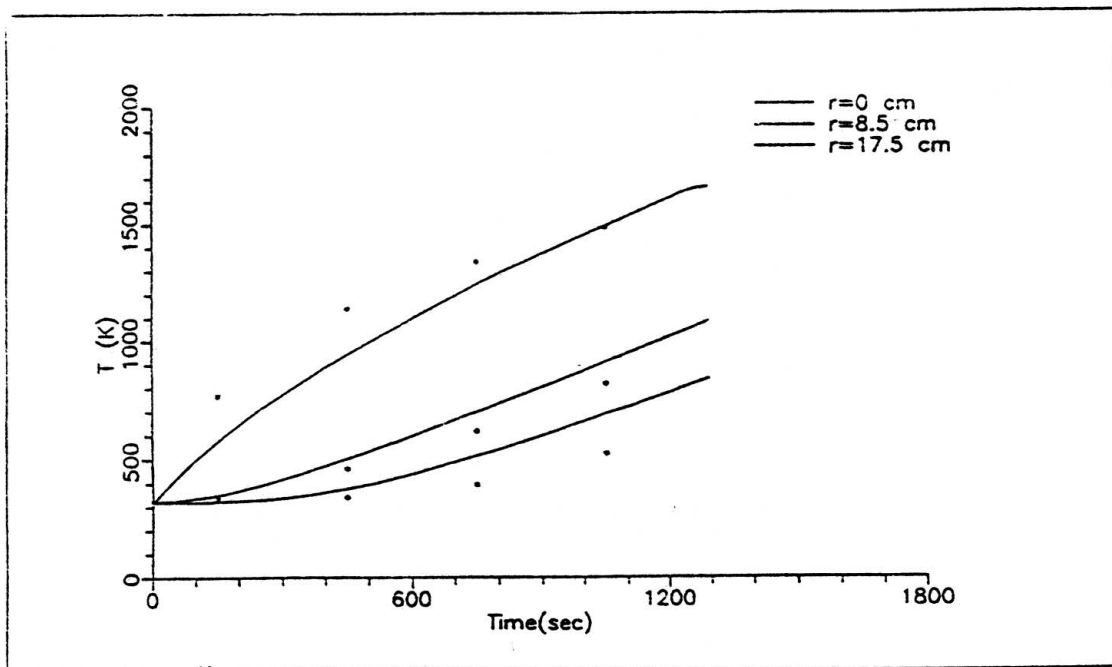


Fig.5.2. Comparison of the calculating results, concerning warming up of the metal cylinder for the calibration experiment

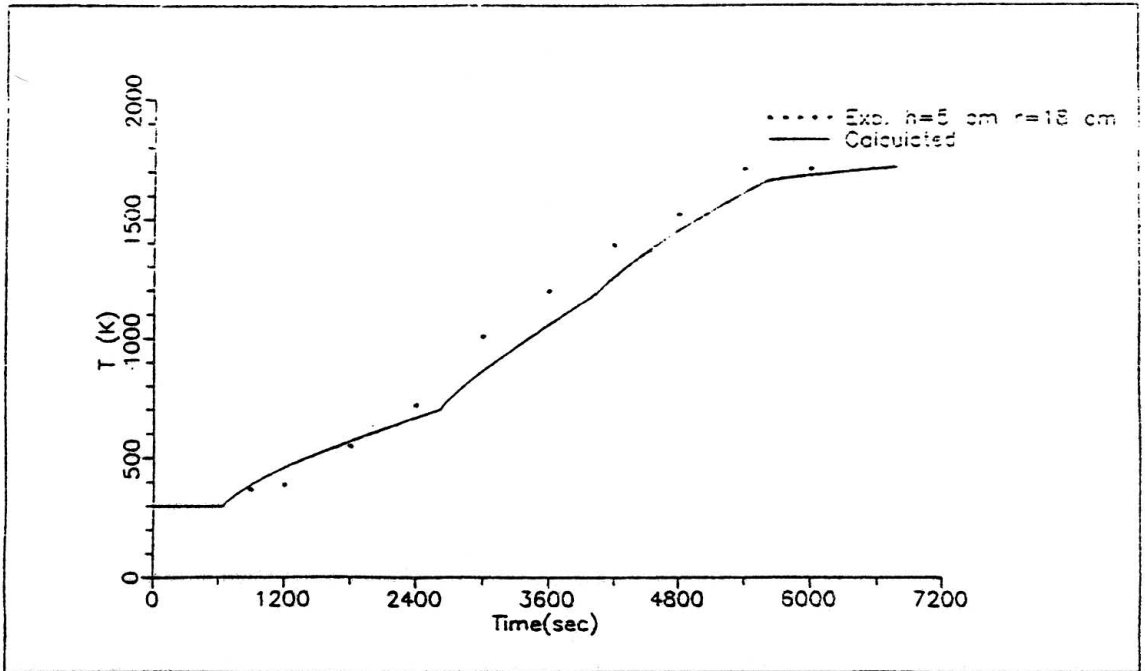


Fig.5.3. Comparison of experimental and measured temperatures in steel on the stage of preliminary heating

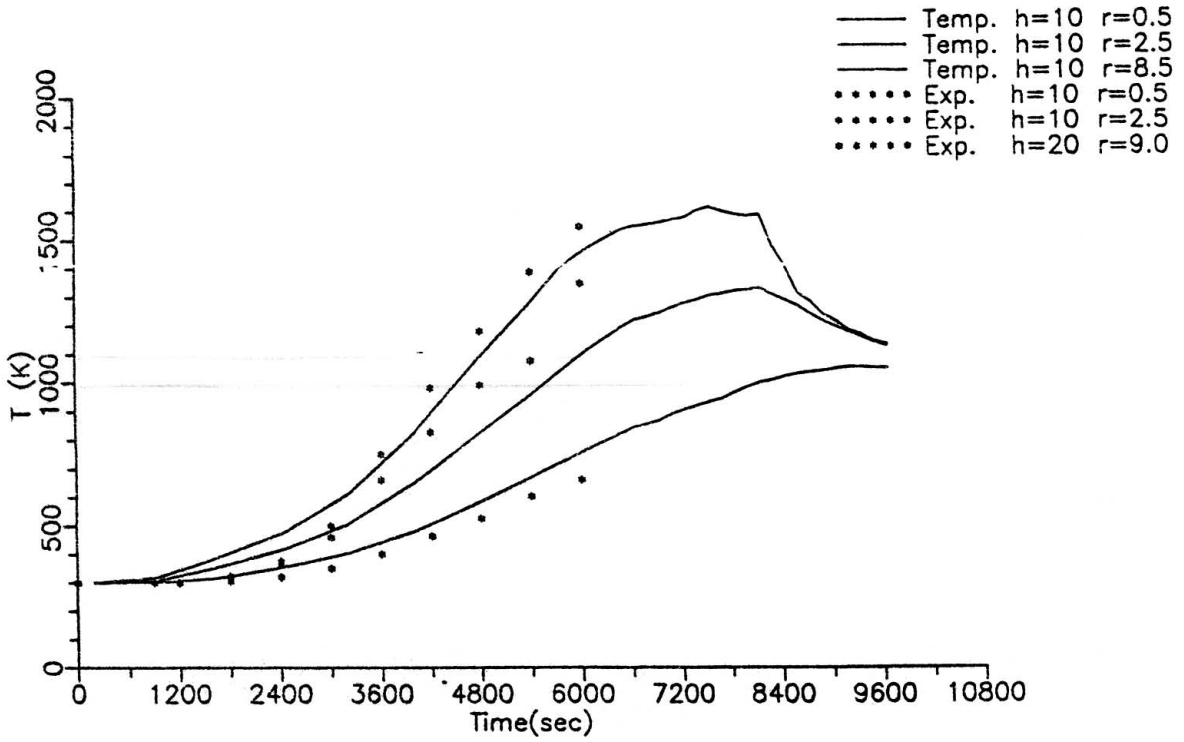


Fig.5.4. Comparison of the experimental and measured temperatures in ceramics on the stage of preliminary heating

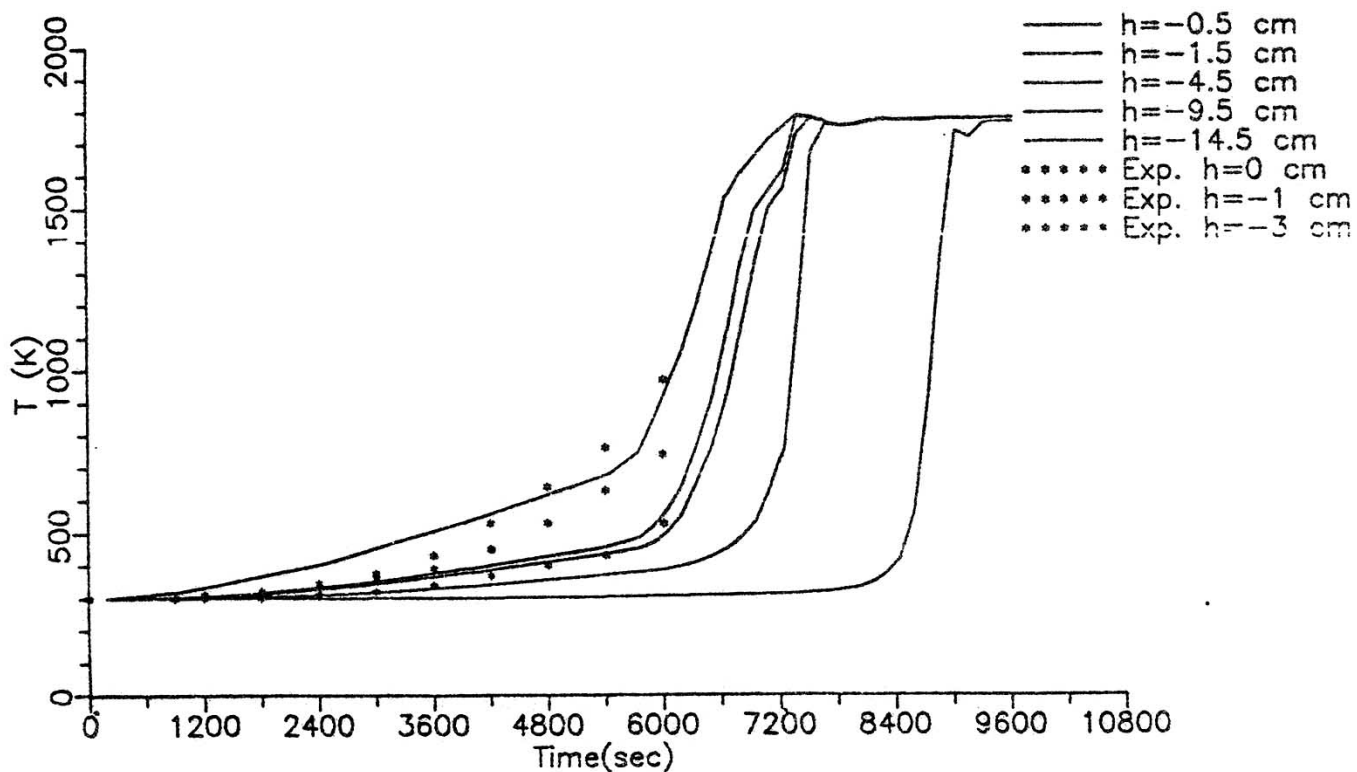


Fig.5.5. Comparison of the experimental and measured temperatures in concrete on the stage of preliminary heating

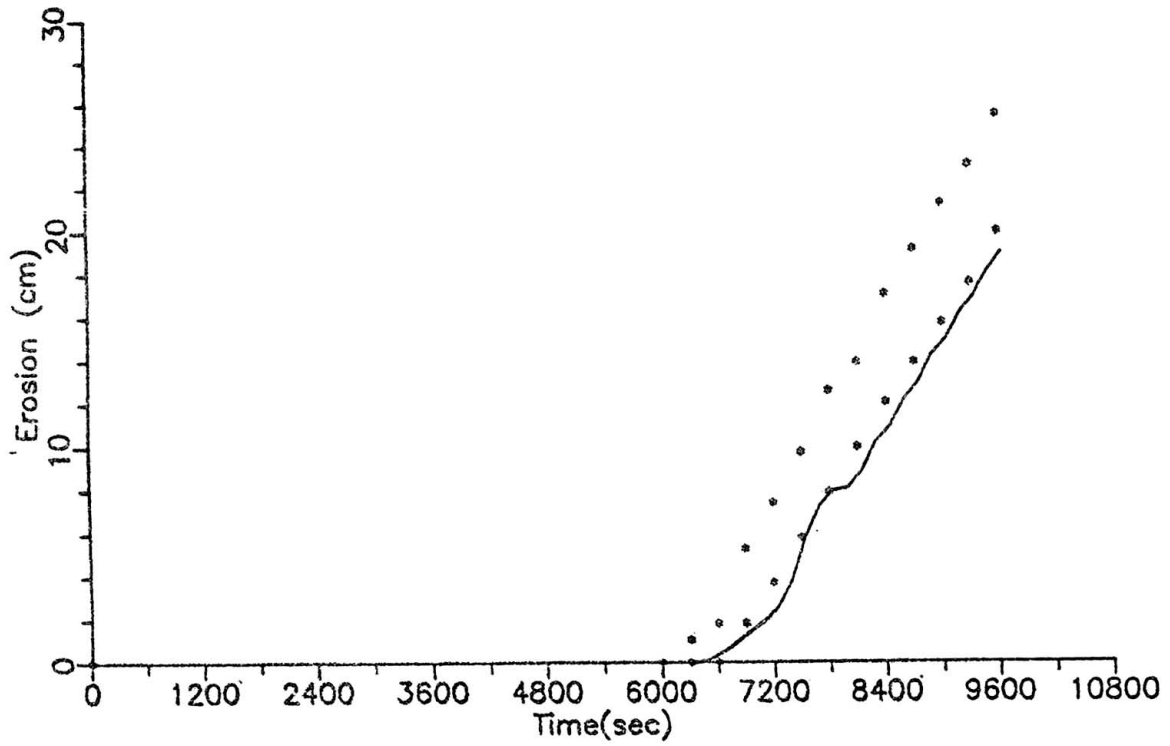


Fig.5.6. The concrete erosion depth, calculated with RA3PLAV code